DOI: 10.3901/CJME.2016.0108.004, available online at www.springerlink.com; www.cjmenet.com

Physical Parameter Identification Method Based on Modal Analysis for Two-axis On-road Vehicles: Theory and Simulation

ZHENG Minyi, ZHANG Bangji*, ZHANG Jie, and ZHANG Nong

State Key Laboratory of Advanced Design and Manufacture for Vehicle Body, Hunan University, Changsha 410082, China

Received August 24, 2015; revised December 16, 2015; accepted January 8, 2016

Abstract: Physical parameters are very important for vehicle dynamic modeling and analysis. However, most of physical parameter identification methods are assuming some physical parameters of vehicle are known, and the other unknown parameters can be identified. In order to identify physical parameters of vehicle in the case that all physical parameters are unknown, a methodology based on the State Variable Method(SVM) for physical parameter identification of two-axis on-road vehicle is presented. The modal parameters of the vehicle are identified by the SVM, furthermore, the physical parameters of the vehicle are estimated by least squares method. In numerical simulations, physical parameters of Ford Granada are chosen as parameters of vehicle model, and half-sine bump function is chosen to simulate tire stimulated by impulse excitation. The first numerical simulation shows that the present method can identify all of the physical parameters and the largest absolute value of percentage error of the identified physical parameter is 0.205%; and the effect of the errors of additional mass, structural parameter and measurement noise are discussed in the following simulations, the results shows that when signal contains 30 dB noise, the largest absolute value of percentage error of the identification is 3.78%. These simulations verify that the presented method is effective and accurate for physical parameter identification of two-axis on-road vehicles. The proposed methodology can identify all physical parameters of 7-DOF vehicle model by using free-decay responses of vehicle without need to assume some physical parameters are known.

Keywords: Parameter identification; free-decay response; state variable method; modal parameter; physical parameter

1 Introduction

Physical parameters of the vehicle play a vital role in the dynamic modeling and analysis of road vehicles, and some of them determine the vehicle handing and ride performance[1–3]. Therefore, many researchers and engineers are interested in physical parameter identification. Several existing methods can measure some of the inertia parameters, such as mass, centre of gravity and mass moments of inertia, by using the Inertial Parameter Measurement Device[4]. These parameters are estimated by four categories of dynamic model: longitudinal, bounce, roll and yaw. Generally, the modal parameter identification is an important part of the physical parameter identification, and this identification method can identify modal parameters of the vehicle, such as natural frequencies, damping ratios and modal shapes. The modal parameter identification methods can be divided into two main categories: (1) frequency domain method, such as peak picking method(P-P), polynomial fitting, maximum likelihood(MLI), PolyMAX method; and (2) time domain method, e.g. Ibrahim Time Domain(ITD), Eigensystem Realization Algorithm(ERA), Auto Regressive Moving Average(ARMA), Empirical Mode Decomposition(EMD), Stochastic Subspace identification(SSI). If adjacent natural frequencies are closed or damping ratios are high, the modal parameters are difficult to be identified by using frequency domain methods. However, time domain methods can still be suitable to identify the modal parameter in such case. Because modal frequencies of vehicle body are in the 1−3Hz range and the corresponding damping ratios are between 0.1 and 0.5, time domain methods would be more appropriate to identify the modal parameters of the vehicle[5].

In recent decades, many parameter identification methods have been proposed to estimate parameters of the on-road vehicle. Kalman filter(KF) method is employed to identify parameters of the vehicle by many researchers. For example, VENHOVENS and NAAB used KF to estimate vehicle system dynamic parameter[6]; RUSSO, et al, presented a methodology based on KF to determine the parameters of a car on the basis of data obtained from standard, on-road handling manoeuvres[7]; HODEGSON and BEST designed a nonlinear KF to identify the real-time lateral and vertical tire force information[8]; WENZEL, et al,

* Corresponding author. E-mail: bangjizhang@hnu.edu.cn
Supported by National Natural Science Foundation of China(Grant Nos. 51175157, U124208)

proposed a dual extended Kalman filter(EKF) technique, which makes use of two KF running in parallel, for vehicle state and parameter estimation[9]; LI, et al, presented a new variable structure EKF for vehicle sideslip angle estimation on a low friction road[10]; ANTONOV, et al, proposed unscented Kalman filter(UKF) for the accurate vehicle state estimation[11]; LI, et al, used a signal fusion method to estimate the comprehensive tire-road friction coefficient of the vehicle under complex maneuvering operations[12]; these kinds of methods need to assume some physical parameters are known and measure input and output signals. However, other parameter identification methodologies also have been developed. For instance, THITE, et al, developed the frequency domain method using a matrix inversion approach for estimating the suspension parameter[13]. KUMAR and SHANKAR used global and substructure approaches in the time domain to identify the parameter of structures with nonlinearities[14]. The online parameter estimation method proposed by ROZYN and ZHANG used the equivalent suspension stiffness coefficient to represent suspension and wheel stations in order to simplify modeling[15]. MEJÍA, et al, presented a method for identification of the inertial parameters of a dynamic front suspension by using inertia and mass transfer to select the potential base parameters, and it would generate well-conditioned models that are very close to the original model behavior[16]. YANG, et al, developed a system identification technique to determine the lateral dynamics of an articulated freight vehicle subject to three different steering excitations and levels of measurement noise[17]. VENTURE, et al, presented a robotics approach, which is based on a multibody dynamic system that allows the automatic computation of the dynamic identification model, to estimate the dynamic parameters of a car[18]. LALTHLAMUANA and TALUKDAR proposed a method combined semi-analytical and particle filtering approach for identification of physical parameters of vehicle from the bridge dynamic response[19]. Based on subspace identification method of modal parameters, DONG et al. proposed a new parameter identification method for estimating roll and pitch moments of inertia of the on-road vehicle[5]. HUH, et al, designed a vehicle mass estimator for adaptive roll stability control[20]. KOULOCHERIS, et al, presented a parametric identification method to estimate structural parameters of commercial passenger vehicle[21]. All of these methods can only identify part of the physical parameters of the vehicle. It is still difficult to identify all physical parameters of the vehicle by using conventional parameter identification methods.

This paper presents a new physical parameter identification method for two-axis on-road vehicle. The State Variable Method (SVM), which is presented by ZHANG and HAYAMA to identify the modal parameter and physical parameter of structural system[22], is employed to identify the modal parameter of vehicle. In order to identify the matrices $\boldsymbol{M}$, $\boldsymbol{C}$ and $\boldsymbol{K}$ of the vehicle, a known additional mass matrix $\Delta\boldsymbol{M}$ is designed to add into the mass matrix of the vehicle in order to increase the number of equations to ensure that the number of equations is more than that of unknowns. Therefore, physical parameters of on-road vehicle can be calculated by using least squares method. To validate the presented method, some numerical simulations are given in this manuscript to discuss the effect caused by the error of additional mass, the error of structural parameter and measurement noise. Numerical simulation results demonstrate that the presented method is effective and accurate for physical parameter identification of a two axis on-road vehicle.

2 Solution Procedures

2.1 Vehicle Dynamic Modeling

A vehicle model shown in Fig. 1 can be described as a system of seven degrees of freedom(DOF), where the sprung mass is assumed to be a rigid body with freedoms of motion in the vertical, pitch and roll direction and each wheel has freedom of motion in vertical direction. In Fig. 1, the mass inertia parameters of vehicle are sprung mass m_s, roll moment of inertia I_{xx}, pitch moment of inertia I_{yy}, unsprung mass m_{ui} (i=A, B, C, D), respectively. c_{si} , k_{si} and k_{ti} (i=A, B, C, D) denote the suspension damping coefficient, the suspension stiffness and the tyre stiffness, respectively. The displacement of vehicle can be denoted by sprung mass vertical translation z_s, the pitch angle θ, the roll angle ϕ, and four vertical translation of wheel z_{ui} (i=A, B, C, D), respectively. The displacements of ground input are denoted by z_{gi} (i=A, B, C, D). a and b represent the distance from the front and rear axle to sprung mass of central gravity (CG). l_f and l_r denote the half width of the front and rear axle, respectively.

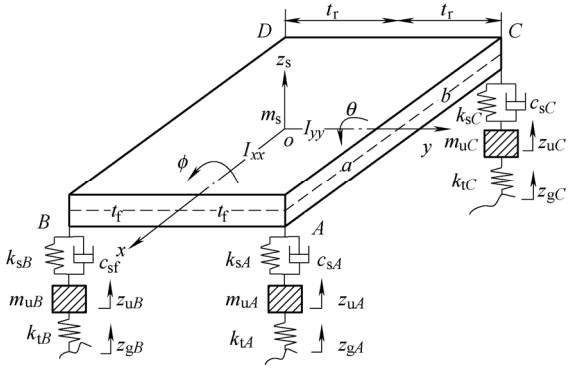

Fig. 1. 7-DOF vehicle model

Based on Newton's law, the dynamic equation of the vehicle system can be derived as follows:

$$\boldsymbol{M}\ddot{\boldsymbol{X}} + \boldsymbol{C}\dot{\boldsymbol{X}} + \boldsymbol{K}\boldsymbol{X} = \boldsymbol{F}, \tag{1}$$

where vectors $\boldsymbol{X}$, $\dot{\boldsymbol{X}}$ and $\ddot{\boldsymbol{X}}$ $\in\mathbf{R}^{7\times1}$ denote the displacement, velocity and acceleration vectors of the vehicle, respectively. $\boldsymbol{M}$, $\boldsymbol{C}$ and $\boldsymbol{K}$ $\in\mathbf{R}^{7\times7}$ are the mass,

damping and stiffness matrices of the vehicle system, and vector $\boldsymbol{F}$ is the road excitation force input of the vehicle.

$$\boldsymbol{X}=(z_{\mathrm{s}},\ \theta,\ \phi,\ z_{\mathrm{u}A},\ z_{\mathrm{u}B},\ z_{\mathrm{u}C},\ z_{\mathrm{u}D})^{\mathrm{T}}, \tag{2}$$

$$\boldsymbol{M}=\mathrm{diag}(m_{\mathrm{s}},\ I_{yy},\ I_{xx},\ m_{\mathrm{u}A},\ m_{\mathrm{u}B},\ m_{\mathrm{u}C},\ m_{\mathrm{u}D}), \tag{3}$$

$$\boldsymbol{C}=\begin{pmatrix}\boldsymbol{L}\boldsymbol{C}_{\mathrm{s}}\boldsymbol{L}^{\mathrm{T}} & -\boldsymbol{L}\boldsymbol{C}_{\mathrm{s}}\\ -\boldsymbol{C}_{\mathrm{s}}\boldsymbol{L}^{\mathrm{T}} & \boldsymbol{C}_{\mathrm{s}}\end{pmatrix}, \tag{4}$$

$$\boldsymbol{K}=\begin{pmatrix}\boldsymbol{L}\boldsymbol{K}_{\mathrm{s}}\boldsymbol{L}^{\mathrm{T}} & -\boldsymbol{L}\boldsymbol{K}_{\mathrm{s}}\\ -\boldsymbol{K}_{\mathrm{s}}\boldsymbol{L}^{\mathrm{T}} & \boldsymbol{K}_{\mathrm{s}}+\boldsymbol{K}_{\mathrm{t}}\end{pmatrix}, \tag{5}$$

$$\boldsymbol{F}=(0,\ 0,\ 0,\ k_{\mathrm{t}A}z_{\mathrm{g}A},\ k_{\mathrm{t}B}z_{\mathrm{g}B},\ k_{\mathrm{t}C}z_{\mathrm{g}C},\ k_{\mathrm{t}D}z_{\mathrm{g}D})^{\mathrm{T}}, \tag{6}$$

where superscript "T" denotes transposition of vector or matrix, and the matrices $\boldsymbol{C}_{\mathrm{s}}$, $\boldsymbol{K}_{\mathrm{s}}$, $\boldsymbol{K}_{\mathrm{t}}$, $\boldsymbol{L}$ are expressed as follows, respectively,

$$\boldsymbol{C}_{\mathrm{s}}=\mathrm{diag}(c_{\mathrm{s}A},\ c_{\mathrm{s}B},\ c_{\mathrm{s}C},\ c_{\mathrm{s}D}), \tag{7}$$

$$\boldsymbol{K}_{\mathrm{s}}=\mathrm{diag}(k_{\mathrm{s}A},\ k_{\mathrm{s}B},\ k_{\mathrm{s}C},\ k_{\mathrm{s}D}), \tag{8}$$

$$\boldsymbol{K}_{\mathrm{t}}=\mathrm{diag}(k_{\mathrm{t}A},\ k_{\mathrm{t}B},\ k_{\mathrm{t}C},\ k_{\mathrm{t}D}), \tag{9}$$

$$\boldsymbol{L}=\begin{pmatrix}1 & 1 & 1 & 1\\ -a & -a & b & b\\ t_{\mathrm{f}} & -t_{\mathrm{f}} & t_{\mathrm{r}} & -t_{\mathrm{r}}\end{pmatrix}. \tag{10}$$

2.2 Modal Parameter Identification based on SVM

Introducing state vector $\boldsymbol{Y}=\{\boldsymbol{X}\quad \dot{\boldsymbol{X}}\}^{\mathrm{T}}$, Eq. (1) can be converted to the state-space equation:

$$\dot{\boldsymbol{Y}}=\boldsymbol{A}\boldsymbol{Y}+\boldsymbol{B}\boldsymbol{F}, \tag{11}$$

where matrices $\boldsymbol{A}$ and $\boldsymbol{B}$ are

$$\boldsymbol{A}=\begin{pmatrix}\boldsymbol{O} & \boldsymbol{I}\\ -\boldsymbol{M}^{-1}\boldsymbol{K} & -\boldsymbol{M}^{-1}\boldsymbol{C}\end{pmatrix}, \tag{12}$$

$$\boldsymbol{B}=\begin{pmatrix}\boldsymbol{O}\\ \boldsymbol{M}^{-1}\end{pmatrix}. \tag{13}$$

The SVM modal parameter identification method relies on the free decay response of vehicle, so it can be assumed that the road excitation input $\boldsymbol{F}$ is zero vector. In the discrete time domain, the state-space equation can be described in the form:

$$\bar{\boldsymbol{\Phi}}=\boldsymbol{A}_{\mathrm{l}}\boldsymbol{\Phi}+\tilde{\boldsymbol{\Phi}}, \tag{14}$$

where $\tilde{\boldsymbol{\Phi}}$ represents an measurement error matrix, and the state matrices $\boldsymbol{\Phi}$ and $\bar{\boldsymbol{\Phi}}$ are defined as

$$\boldsymbol{\Phi}=\big(\boldsymbol{Y}(1),\ \boldsymbol{Y}(2),\ \cdots,\ \boldsymbol{Y}(N)\big), \tag{15}$$

$$\bar{\boldsymbol{\Phi}}=\big(\boldsymbol{Y}(2),\ \boldsymbol{Y}(3),\ \cdots,\ \boldsymbol{Y}(N+1)\big), \tag{16}$$

$$\boldsymbol{Y}(k)=(\boldsymbol{X}^{\mathrm{T}}(k),\ \boldsymbol{X}^{\mathrm{T}}(k+1),\ \cdots,\ \boldsymbol{X}^{\mathrm{T}}(k+p))^{\mathrm{T}}, \tag{17}$$

where $\boldsymbol{Y}(k)$ is the discrete vector of measurement, N is the number larger than the rank of state matrix $\boldsymbol{\Phi}$, $\boldsymbol{X}(k)$ represents the sensor measurements at $t=k\Delta T$, p is the parameter determined by the number of degrees of freedom, the number of measurement points and the signal to noise ratio of measurement. The transition matrix $\boldsymbol{A}_{\mathrm{l}}$ can be determined by using least squares method and can be expressed as

$$\boldsymbol{A}_{\mathrm{l}}=(\bar{\boldsymbol{\Phi}}\boldsymbol{\Phi}^{\mathrm{T}})(\boldsymbol{\Phi}\boldsymbol{\Phi}^{\mathrm{T}})^{-1}. \tag{18}$$

Solving the eigenvalue problem of the transition matrix $\boldsymbol{A}_{\mathrm{l}}$ gives the eigenvalues z_i and eigenvectors $\boldsymbol{P}_i$ (i=1, 2,⋯, 7) on the Z plane.

On the other hand, based on the relation between the continuous system and the discrete system, the transition matrix $\boldsymbol{A}_{\mathrm{l}}$ can be expressed as follows:

$$\boldsymbol{A}_{\mathrm{l}}=\exp(\boldsymbol{A}\Delta T), \tag{19}$$

where ΔT is the sampling interval.

Therefore, the eigenvalues λ_i and eigenvectors $\boldsymbol{\Phi}_i$ of state matrix $\boldsymbol{A}$ can be calculated as follows:

$$\lambda_i=\ln z_i/\Delta T, \tag{20}$$

$$\boldsymbol{\Phi}_{\boldsymbol{i}}=\boldsymbol{P}_{\boldsymbol{i}},\ (i=1,\ 2,\cdots,\ 7). \tag{21}$$

2.3 Physical Parameter Identification

Once the eigenvalues and eigenvectors of state matrix $\boldsymbol{A}$ are obtained, the identification state matrix $\boldsymbol{A}_{\mathrm{id}}$ can be calculated through the following formula:

$$\boldsymbol{A}_{\mathrm{id}}=\begin{pmatrix}\boldsymbol{\Phi} & \boldsymbol{\Phi}^{*}\\ \boldsymbol{\Phi}\boldsymbol{\Lambda} & \boldsymbol{\Phi}^{*}\boldsymbol{\Lambda}^{*}\end{pmatrix}\begin{pmatrix}\boldsymbol{\Lambda} & \\ & \boldsymbol{\Lambda}^{*}\end{pmatrix}\begin{pmatrix}\boldsymbol{\Phi} & \boldsymbol{\Phi}^{*}\\ \boldsymbol{\Phi}\boldsymbol{\Lambda} & \boldsymbol{\Phi}^{*}\boldsymbol{\Lambda}^{*}\end{pmatrix}^{-1}, \tag{22}$$

where

$$\boldsymbol{\Lambda}=\mathrm{diag}(\lambda_1,\ \lambda_2,\ \cdots,\ \lambda_7), \tag{23}$$

$$\boldsymbol{\Phi}=\big(\boldsymbol{\Phi}_1,\ \boldsymbol{\Phi}_2,\ \cdots,\ \boldsymbol{\Phi}_7\big), \tag{24}$$

$\boldsymbol{\Lambda}^{*}$ and $\boldsymbol{\Phi}^{*}$ are the conjugate matrices of $\boldsymbol{\Lambda}$ and $\boldsymbol{\Phi}$, respectively.

It can be found that the number of equations are less than

that of unknowns in Eq. (12). So the mass matrix $\boldsymbol{M}$, the damping coefficient matrix $\boldsymbol{C}$ and the stiffness matrix $\boldsymbol{K}$ of the vehicle cannot be determined by solving Eq. (12). To make it possible to calculate matrices $\boldsymbol{M}$, $\boldsymbol{C}$ and $\boldsymbol{K}$ of the vehicle, a known mass matrix $\Delta\boldsymbol{M}$ is added into the vehicle system to increase the number of equations. Then, the new state matrix $\bar{\boldsymbol{A}}$ of vehicle with additional mass can be expressed as

$$\bar{\boldsymbol{A}}=\begin{pmatrix}\boldsymbol{O} & \boldsymbol{I}\\ -(\boldsymbol{M}+\Delta\boldsymbol{M})^{-1}\boldsymbol{K} & -(\boldsymbol{M}+\Delta\boldsymbol{M})^{-1}\boldsymbol{C}\end{pmatrix}. \tag{25}$$

Combining Eqs. (12) and (25), the number of equations is more than that of the unknowns. Let $\boldsymbol{A}_{21}$ and $\boldsymbol{A}_{22}$ denote the sub-matrices of state matrix $\boldsymbol{A}$, $\bar{\boldsymbol{A}}_{21}$ and $\bar{\boldsymbol{A}}_{22}$ denote the sub-matrices of state matrix $\bar{\boldsymbol{A}}$. The expressions of sub-matrices $\boldsymbol{A}_{21}$, $\boldsymbol{A}_{22}$, $\bar{\boldsymbol{A}}_{21}$ and $\bar{\boldsymbol{A}}_{22}$ are, respectively,

$$\boldsymbol{A}_{21}=-\boldsymbol{M}^{-1}\boldsymbol{K}, \tag{26}$$

$$\boldsymbol{A}_{22}=-\boldsymbol{M}^{-1}\boldsymbol{C}, \tag{27}$$

$$\bar{\boldsymbol{A}}_{21}=-(\boldsymbol{M}+\Delta\boldsymbol{M})^{-1}\boldsymbol{K}, \tag{28}$$

$$\bar{\boldsymbol{A}}_{22}=-(\boldsymbol{M}+\Delta\boldsymbol{M})^{-1}\boldsymbol{C}. \tag{29}$$

Since the damping coefficient matrix $\boldsymbol{C}$ of the vehicle is a singular matrix, and the sub-matrices $\boldsymbol{A}_{22}$ and $\bar{\boldsymbol{A}}_{22}$ contain the damping coefficient matrix $\boldsymbol{C}$, so the inverse matrices of $\boldsymbol{A}_{22}$ and $\bar{\boldsymbol{A}}_{22}$ cannot be determined. However, the stiffness matrix $\boldsymbol{K}$, and the sub-matrices $\boldsymbol{A}_{21}$ and $\bar{\boldsymbol{A}}_{21}$ are non-singular matrices. Therefore, the mass matrix $\boldsymbol{M}$ can only be calculated by Eqs. (26) and (28). Then, the mass matrix $\boldsymbol{M}$ of the vehicle can be calculated as

$$\boldsymbol{M}=\Delta\boldsymbol{M}\bar{\boldsymbol{A}}_{21}(\boldsymbol{A}_{21}-\bar{\boldsymbol{A}}_{21})^{-1}. \tag{30}$$

Once the mass matrix $\boldsymbol{M}$ is obtained, the damping coefficient matrix $\boldsymbol{C}$ can be determined by solving Eq. (27) or (29). The coefficient matrix $\boldsymbol{C}$ can be expressed as

$$\boldsymbol{C}=-\Delta\boldsymbol{M}\bar{\boldsymbol{A}}_{21}(\boldsymbol{A}_{21}-\bar{\boldsymbol{A}}_{21})^{-1}\boldsymbol{A}_{22}, \tag{31}$$

or

$$\boldsymbol{C}=-\Delta\boldsymbol{M}(\bar{\boldsymbol{A}}_{21}(\boldsymbol{A}_{21}-\bar{\boldsymbol{A}}_{21})^{-1}\bar{\boldsymbol{A}}_{22}+\bar{\boldsymbol{A}}_{22}). \tag{32}$$

Similarly, the stiffness matrix $\boldsymbol{K}$ can be obtained by solving Eq. (26) or Eq. (28):

$$\boldsymbol{K}=-\Delta\boldsymbol{M}\bar{\boldsymbol{A}}_{21}(\boldsymbol{A}_{21}-\bar{\boldsymbol{A}}_{21})^{-1}\boldsymbol{A}_{21}. \tag{33}$$

If $\boldsymbol{A}_{21}$, $\boldsymbol{A}_{22}$, $\bar{\boldsymbol{A}}_{21}$ and $\bar{\boldsymbol{A}}_{22}$ are chosen to be the sub-matrix of the state matrix $\boldsymbol{A}$ and $\bar{\boldsymbol{A}}$ identified by SVM, the matrices $\boldsymbol{M}$, $\boldsymbol{C}$ and $\boldsymbol{K}$ of the vehicle can be calculated through Eqs. (30)–(33). Furthermore, all of physical parameter of the vehicle including the mass inertia parameters, suspension damping coefficients, suspension stiffnesses and tyre stiffnesses can be determined by using least squares method.

3 Numerical Simulations

3.1 Simulation of the road-tyre excitation

In the 7-DOF vehicle model, the excitations of the vehicle system are four road-tyre excitations including $k_{tA}z_{gA}$, $k_{tB}z_{gB}$, $k_{tC}z_{gC}$ and $k_{tD}z_{gD}$. In order to obtain the free decay response of the vehicle, the half-sine bump z_g can be chosen as the road input functions, and the excitations z_{gA}, z_{gB}, z_{gC} and z_{gD} are used for simulating the tires stimulated by impulse excitation. Assume the function of z_g can be described as follows:

$$z_g(t)=\begin{cases}0.09\sin(5\pi(t-0.1)), & 0.1\leqslant t\leqslant 0.3,\\ 0, & t<0.1 \text{ or } t>0.3.\end{cases} \tag{34}$$

For the 7-DOF vehicle model, there are seven body-wheel motion modes. These motion modes can be classified as two groups: the body-dominated and wheel-dominated motion mode. Three body-dominated motion modes are body-dominated bounce mode, body-dominated pitch mode and body-dominated roll mode, respectively. In general, their frequencies are range between 1 and 3 Hz, and vehicle body has much larger displacement than wheels in their mode shapes. Four wheel-dominated motion modes are wheel-dominated bounce mode, wheel-dominated pitch mode, wheel-dominated roll mode and wheel-dominated warp mode, respectively. Generally, their frequencies are range between 10 to 15 Hz, and vehicle body has much smaller displacement than wheels in their mode shapes. According to the vibration characteristic of the body-wheel motion modes of the vehicle, the numerical simulations are divided into three cases:

(1) Bounce mode excitation, four road input function z_{gA}, z_{gB}, z_{gC} and z_{gD} are both equal to z_g;

(2) Pitch mode excitation, the front road input function (z_{gA}, z_{gB}) or the rear road input function(z_{gC}, z_{gD}) are equal to z_g;

(3) Roll mode excitation, the left road input function(z_{gA}, z_{gC}) or the right road input function(z_{gB}, z_{gD}) are equal to z_g.

The purpose of these mode excitations is to concentrate the excitation energy to stimulate the relative mode vibration.

3.2 Physical parameters of vehicle model

A Ford Granada is chosen as a vehicle case in numerical simulations. The physical parameters of Ford Granada are listed in Table 1. All the parameters in Table 1 are given in

Ref. [3].

Table 1. Physical parameters of Ford Granada

Parameter	Value
Sprung mass m_s/kg	1380
Sprung mass inertia of the pitch I_{yy}/(kg • m^2)	2440
Sprung mass inertia of the roll I_{xx}/(kg • m^2)	380
Unsprung mass of the front m_{uf}/kg	40.5
Unsprung mass of the rear m_{ur}/kg	45.4
Suspension stiffness of the front k_{sf}/(kN • m^{-1})	17
Suspension stiffness of the rear k_{sr}/(kN • m^{-1})	22
Tire stiffness of the front k_{tf}/(kN • m^{-1})	192
Tire stiffness of the rear k_{tr}/(kN • m^{-1})	192
Suspension damping coefficient of the front c_{sf}/(kN • s • m^{-1})	1.5
Suspension damping coefficient of the rear c_{sr}/(kN • s • m^{-1})	1.5
Distance from the sprung mass CG to the front axle a/m	1.25
Distance from the sprung mass CG to the rear axle b/m	1.51
Half width of the front axle t_f/m	0.74
Half width of the rear axle t_r/m	0.74

3.3 Identification Results

How to choose the additional mass would affect the accuracy of physical parameter identification. Fig. 2 shows the relationship between the relative variation of modal parameter with the incremental percentage of mass. With the incremental percentage of mass varying from 2% to 14%, the relative variety of modal parameters range from –0.98% to –6.8%. If the incremental percentage of mass is less than 10%, the decreasing percentage of modal parameter is less than 5%. Considering the measurement signal contains noise, if the incremental percentage of mass is too small, it will cause large physical parameter identification error of the vehicle. It is suggested that the incremental percentage of mass should be over 10% in order to achieve better identification accuracy. In this manuscript, it is assumed the additional mass $\Delta\boldsymbol{M}$ is as follows:

$$\Delta\boldsymbol{M} = \mathrm{diag}(130,\ 250,\ 40,\ 4,\ 4,\ 5,\ 5). \tag{36}$$

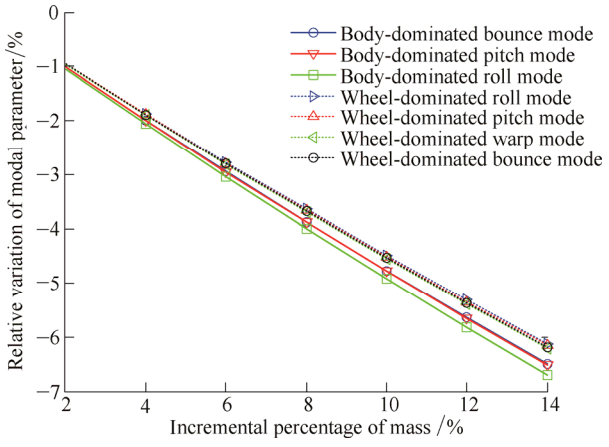

Fig. 2 Relationship between the relative variation of the modal parameter with the incremental percentage of mass

In numerical simulation, Wilson-theta method is employed to calculate the acceleration responses of the vehicle stimulated by the road-tyre excitation. In the physical parameter identification procedures, all physical parameter of vehicle are identified and listed in Table 2. It shows the comparison of the parameters of identification with the ones of vehicle, the largest absolute percentage error of identification is 0.205%. It proves that the theory of presented method is correct and effective for identifying physical parameter of the vehicle.

Table 2. Comparison the parameters of identification with the ones of vehicle

Notation	Known	Identified	Percentage error/%
M_s	1380	1379.85	–0.011
I_{yy}	2440	2439.73	–0.011
I_{xx}	380	379.91	–0.023
m_{uf}	40.5	40.54	0.093
m_{ur}	45.4	45.44	0.095
k_{sf}	17 000	16 971.05	–0.170
k_{sr}	22 000	21 982.85	–0.078
k_{tf}	192 000	191 932.79	–0.039
k_{tr}	192 000	191 938.46	–0.032
c_{sf}	1500	1498.45	–0.103
c_{sr}	1500	1498.70	–0.087
a	1.25	1.282	–0.141
b	1.51	1.508	–0.130
t_f	0.74	0.738	–0.205
t_r	0.74	0.739	–0.161

4 Discussion

4.1 Effect of the error of additional mass

In practical problem, the additional mass may contain some errors caused by weigh or measurement. Therefore, it is necessary to discuss the parameter identification affected by the error of additional mass. For the convenience of discussion, physical parameters of the vehicle are divided into inertia parameters: m_s, I_{yy}, I_{xx}, m_{uA}, m_{uB}, m_{uC}, m_{uD}; dynamic parameters: k_{sf}, k_{sr}, k_{tf}, k_{tr}, c_{sf}, c_{sr}; and structural parameters: a, b, t_f, t_r. In current study, the inertia parameters are identified firstly through Eq. (30); then, the dynamic parameters are calculated by using the elements of matrices $\boldsymbol{C}$ and $\boldsymbol{K}$, which only contain the dynamic parameters; finally, the structural parameters are determined by using the elements of matrix $\boldsymbol{K}$, which only contain the linear term of structural parameters. Eq. (30) shows that the mass matrix $\boldsymbol{M}$ is proportional to the additional matrix $\Delta\boldsymbol{M}$, thus the percentage error of mass matrix caused by the error of additional mass is proportional to the error of additional mass. Figs. 3–7 show the percentage errors of identified dynamic parameters and identified structural parameters affected by the errors of Δm_s, ΔI_{yy}, ΔI_{xx}, Δm_{uf} and Δm_{ur}, respectively. Fig. 3 shows that the error of Δm_s can obviously affects the accuracy of parameters k_{sf}, k_{sr}, c_{sf}, c_{sr}, a, b, t_f and t_r. When the percentage error of Δm_s increases from –5% to 5%, the percentage errors of identification parameters k_{sf}, k_{sr}, c_{sf} and

c_{sr} decrease linearly from about 4% to –4%, and the percentage error of identification structural parameter increases proportionally from about –5% to 5%. However, the effect of parameters k_{tf} and k_{tr} is very small. Figs. 4 and 5 show that the error of additional pitch moment inertia and roll moment inertia will not affect the accuracy of dynamic parameters and they only affect corresponding structural parameters. When the percentage error of moment inertia increases from –5% to 5%, the percentage error of structural parameter decreases linearly from about 2.4% to –2.6%. Figs. 6 and 7 show that the error of additional unsprung mass can affect all of the dynamic parameters and structural parameters. With the increasing of the percentage error of additional unsprung mass from –5% to 5%, the largest absolute value of the percentage error of dynamic parameter and structural parameter is about 5.6% and the effect of the parameters k_{tf} and k_{tr} is more obvious than that of parameters k_{sf}, k_{sr}, c_{sf} and c_{sr}.

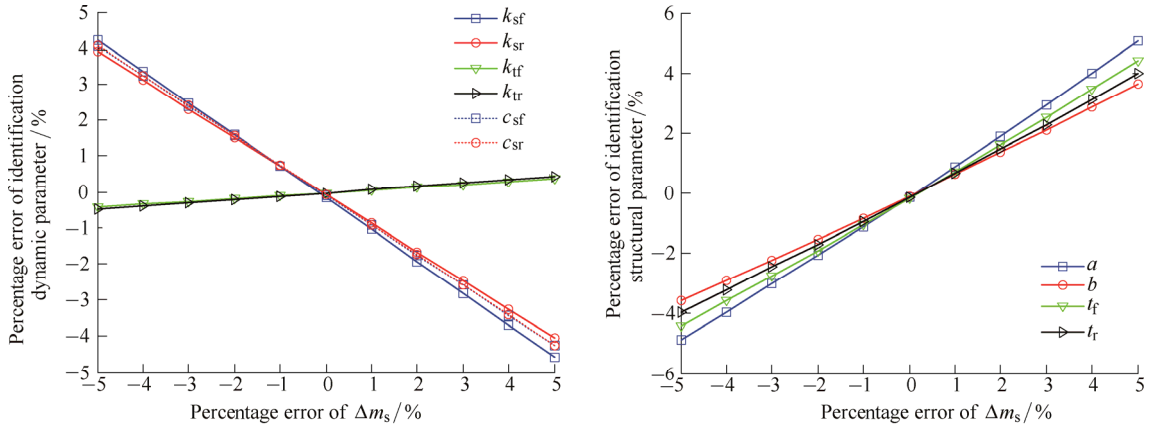

(a) (b)

Fig. 3 Identification of parameter affected by the percentage error of Δm_s

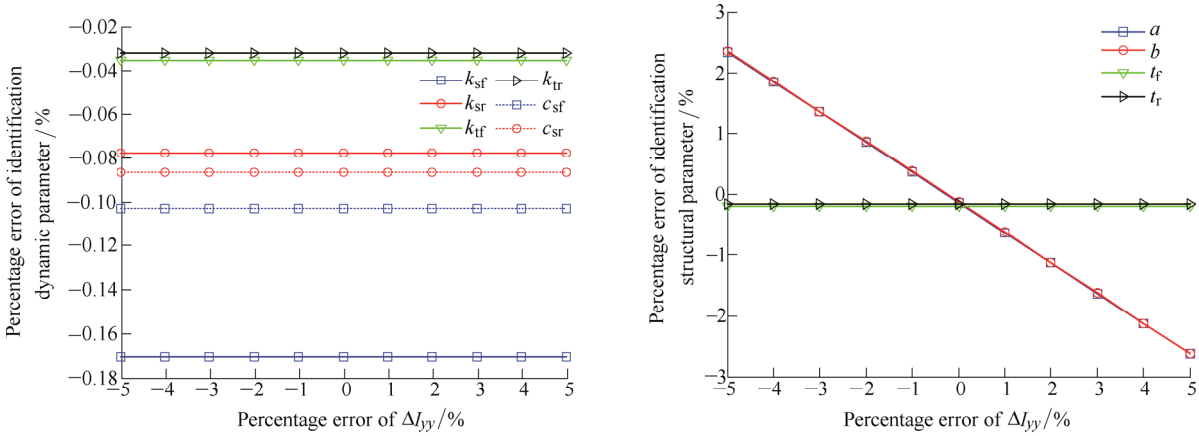

(a) (b)

Fig. 4 Identification of parameter affected by the percentage error of ΔI_{yy}

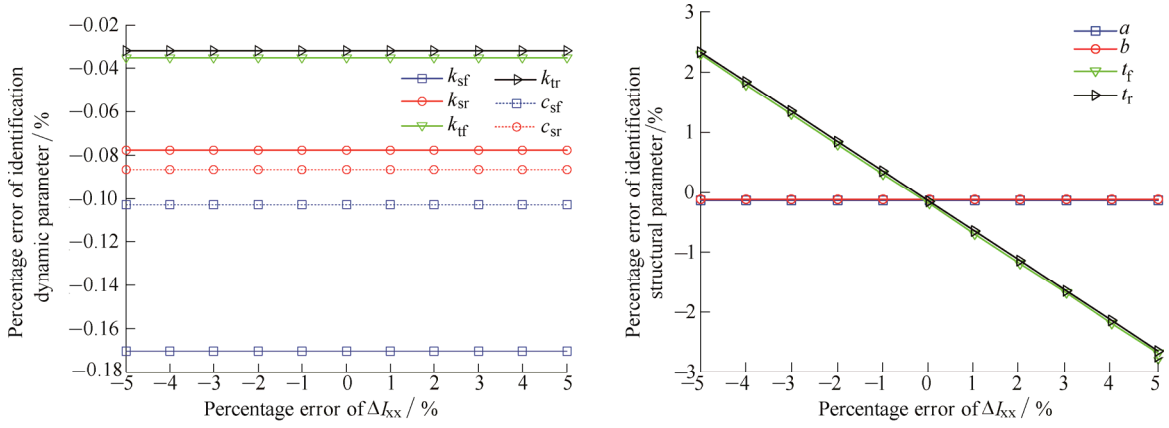

(a) (b)

Fig. 5 Identification of parameter affected by the percentage error of ΔI_{xx}

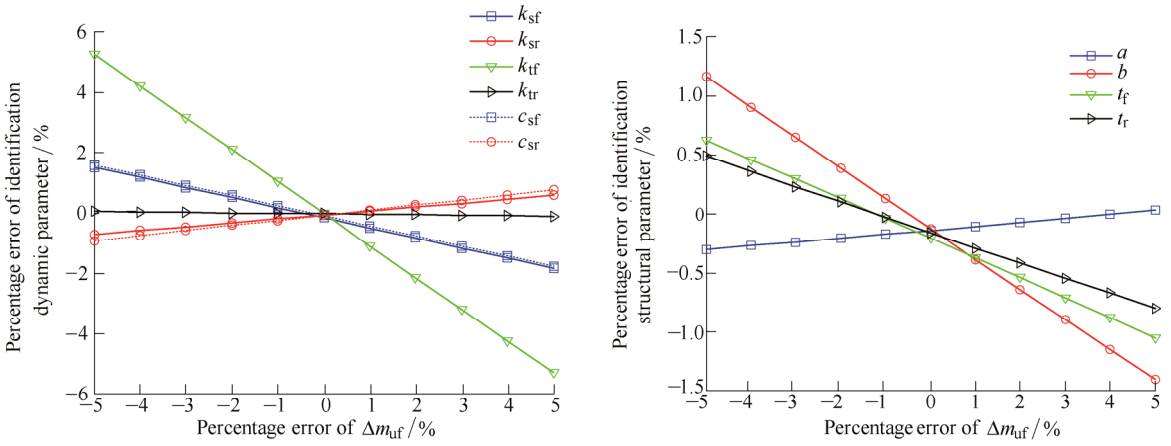

Fig. 6 Identification of parameter affected by the percentage error of Δm_{uf}

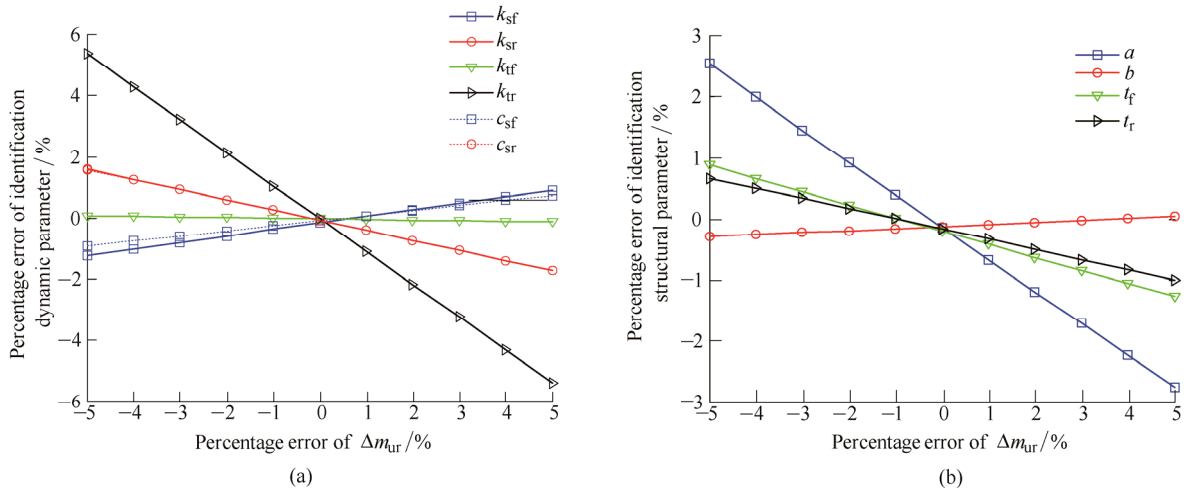

Fig. 7 Identification of parameter affected by the percentage error of Δm_{ur}

4.2 Effect of the Error of Structural Parameter

The structural parameter can also be obtained directly or indirectly through measurement. For example, the parameters t_f and t_r can be measured directly, and the parameters a and b can be calculated by using the relationship between the front and rear axle loads. These structural parameters may contain some measurement errors and the effect of the error of structural parameter in the physical parameter identification will be discussed in this section. The inertia parameters are also calculated by using Eq. (30), after that, the dynamic parameters are calculated by using the elements of matrices $\boldsymbol{C}$ and $\boldsymbol{K}$. Eq. (30) illustrates that the inertia parameters only relate to additional mass and the sub-matrix of identification state matrices. Therefore, the error of structural parameter will not affect the identification of inertia parameters. Fig. 8 presents how the dynamic parameters are affected by the error of structural parameter. It shows that the effect of the parameters a and b is significantly bigger than that of the parameters t_f and t_r. Furthermore, the effect of parameters k_{tf} and k_{tr} caused by the error of structural parameters is very small. The percentage error of identified dynamic parameters is approximately linear with the percentage error of structural parameters. When the percentage error of structural parameters a and b increases from –5% to 5%, the percentage errors of identified parameters k_{sf} and c_{sf} increase from about –4.8% to 4.7%, and the ones of identification parameters k_{sr} and c_{sr} increase from about –5.8% to 5.9%. When the percentage error of parameters t_f increases from –5% to 5%, the percentage errors of identified parameters k_{sf} and c_{sf} increase from about –0.74% to 4%. When the percentage error of parameters t_r increases from –5% to 5%, the percentage errors of identification parameters k_{sf}, k_{sr} and c_{sr} increase from about –0.48% to 0.25%, and the ones of identified parameter c_{sf} increase from about –0.35% to 0.15%. Since the rear suspension stiffness k_{sr} is larger than the front suspension stiffness k_{sf}, the error of t_r can affect both the front and rear suspension dynamic parameters significantly.

4.3 Effect of Noise

The real response of the vehicle is measured by sensors such as displacement sensor, acceleration sensor and gyroscope. It is inevitable that the measured signal contains noise. This section will discuss the effect of noise. The 30 dB noise is added into the simulation in order to simulate the real vehicle response. The MATLAB *firls* function is the linear-phase FIR filter function designed by using

least-squares error minimization. This filter function is employed to filter the signal contained noise. Since the frequencies of the vehicle are between 1 to 15 Hz, the low pass filter is selected to filter, and the pass band cutoff frequency is chosen as 16 Hz. Fig. 9 shows that the comparison between the filtered signal and the signal contained noise. In the parameter identification procedure, the structural parameters are obtained by measurement. Table 3 shows the comparison of the parameters of identification with the values of vehicle. It illustrates that the noise indeed affects the accuracy of the identification. Although the low pass filter has filtered the high-frequency noise, the low-frequency noise signal can still affect the modal parameter identification. Furthermore, the physical parameters are also affected by the low-frequency noise. The largest absolute value of the percentage error of the identification is 3.784%. It demonstrates that the present method can be applied to identify the physical parameter, even the vehicle system contains 30 dB noise signal.

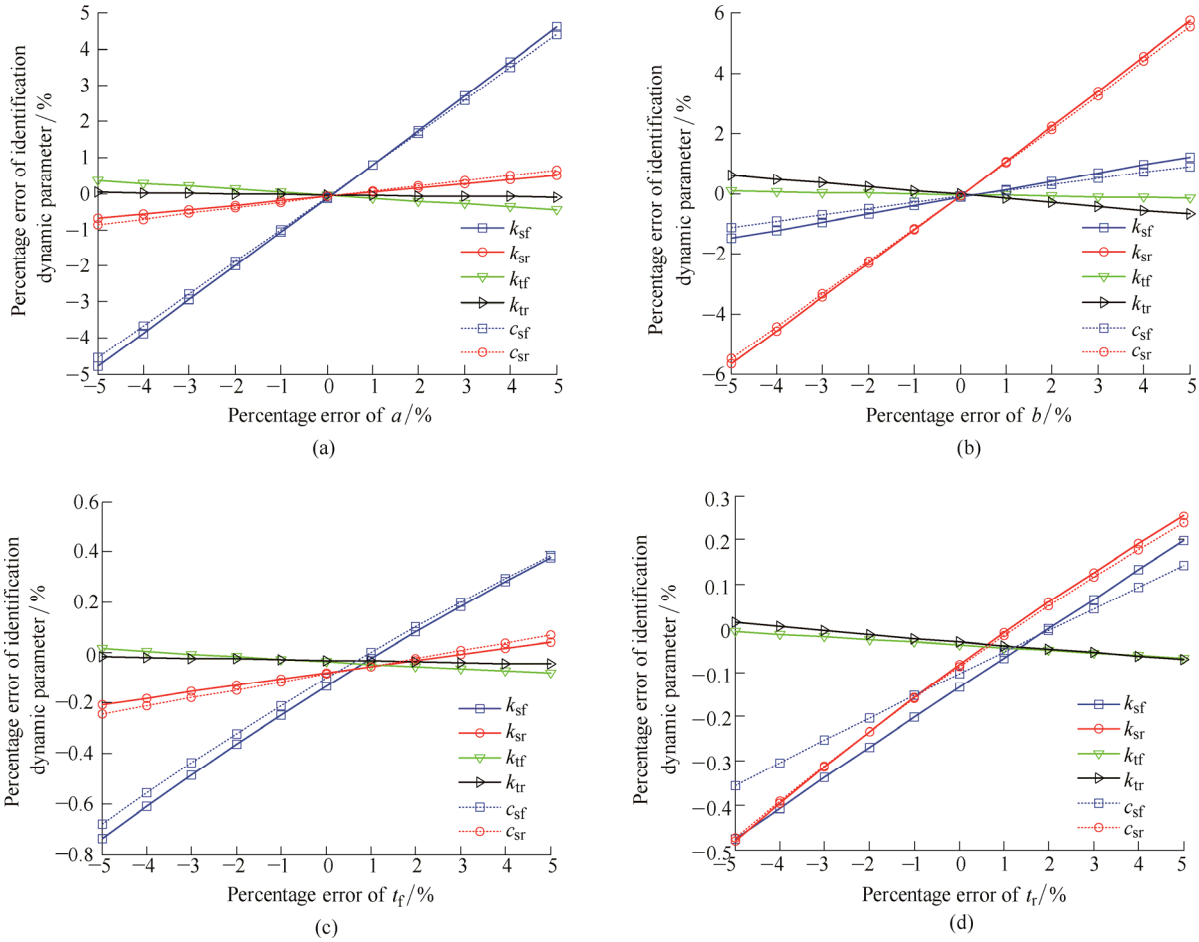

Fig. 8 Identification dynamic parameter affect by the error of structural parameter

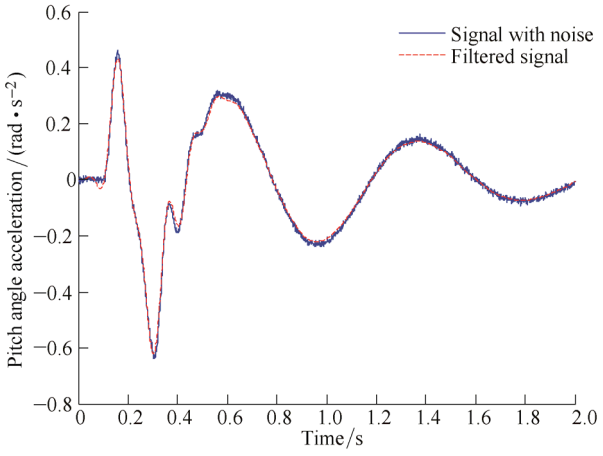

Fig. 9 Comparison the filtered signal with the signal contained noise

Table 3. Comparison the parameters of identification with the ones of vehicle

Notation	Known	Identified	Percentage error / %
M_s	1380	1348.17	–2.307
I_{yy}	2440	2526.28	3.536
I_{xx}	380	368.91	–2.918
m_{uf}	40.5	41.28	1.928
m_{ur}	45.4	44.32	–2.379
k_{sf}	17 000	17271.05	1.594
k_{sr}	22 000	21167.61	–3.784
k_{tf}	192 000	187 684.01	–2.248
k_{tr}	192 000	194 985.47	1.555
c_{sf}	1500	1445.30	–3.647
c_{sr}	1500	1534.06	2.271

5 Conclusions

(1) A new physical parameter identification method based on the State Variable Method for two-axis vehicles has been presented. The modal parameters of vehicle are identified by using SVM. Furthermore, the physical parameters of vehicle are estimated by least squares method.

(2) A numerical simulation example given in this paper shows that the presented method can effectively identify all physical parameters of the vehicle from the free decay responses of vehicle.

(3) The sensitivity investigation results demonstrate that even if the practical problem caused by measurement exists, the presented method is still effective for vehicle parameter identification.

References

[1] GILLESPIE T D. *Fundamentals of vehicle dyamaics*[M]. Warrendale, PA: SAE Inc., 1992.

[2] KIM J. Analysis of handling performance based on simplified lateral vehicle dynamics[J]. *International Journal of Automotive and Technology*, 2008, 9(6): 687–693.

[3] TCHAMNA R, YOUN I. Yaw rate and side-slip control considering vehicle longitudinal dynamics[J]. *International Journal of Automotive and Technology*, 2013, 14(1): 53–60.

[4] GARROTT W, MONK M, CHRSTOS J. Vehicle inertial parameters—measured values and approximations[J]. *SAE Technical Paper Series*, 1988: 881767.

[5] DONG G M, CHEN J, ZHANG N. Investigation into on-road vehicle parameter identification based on subspace methods[J]. *Journal of Sound and Vibration*, 2014, 333(24): 6760–6779.

[6] VENHOVENS P J TH, NAAB K. Vehicle dynamics estimation using kalman filters[J]. *Vehicle System Dynamics*, 1999, 32: 171–184.

[7] RUSSO M, RUSSO R, VOLPE A. Car parameters identification by handling manoeuvres[J]. *Vehicle System Dynamics*, 2000, 34: 423–436.

[8] HODEGSON G, BEST M C. A parameter identifying a Kalman filter observer for vehicle handling dynamics[J]. *Proceedings of the Institution of Mechanical Engineers Part D: Journal of Automobile Engineering*, 2006, 220(8): 1063–1072.

[9] WENZEL T A, BURNHAM K J, BLUNDELL M V, et al. Dual extended Kalman filter for vehicle state and parameter estimation[J]. *Vehicle System Dynamics*, 2006, 44(2): 153–171.

[10] LI L, JIA G, RAN X, et al. A variable structure extended Kalman filter for vehicle sideslip angle estimation on a low friction road[J]. *Vehicle System Dynamics*, 2014, 52(2): 280–308.

[11] ANTONOV S, FEHN A, KUGI A. Unscented Kalman filter for vehicle state estimation[J]. *Vehicle System Dynamics*, 2011, 49(9): 1497–1520.

[12] LI L, YANG K, JIA G, et al. Comprehensive tire-road friction coefficient estimation based on signal fusion method under complex maneuvering operations[J]. *Mechanical Systems and Signal Processing*, 2015, 56(57): 259–276.

[13] THITE A N, BANVIDI S, IBICEK T, et al. Suspension parameter estimation in the frequency domain using a matrix inversion approach[J]. *Vehicle System Dynamics*, 2011, 49(2): 1803–1822.

[14] KUMAR R K, SHANKAR K. Parametric identification of structures with nonlinearities using global and substructure approaches in the time domain[J]. *Advances in Structural Engineering*, 2009, 12: 95–210.

[15] ROZYN M, ZHANG N. A method for estimation of vehicle inertial parameters[J]. *Vehicle System Dynamic*, 2010, 48: 547–565.

[16] MEJÍA L, MATA V, VALERO F, et al. Dynamic parameter identification in the front suspension of a vehicle: On the influence of different base parameter sets[J]. *Multibody Mechatronic Systems*, 2015, 25: 165–175.

[17] YANG X, RAKHEJA S, STIHARU I. Identification of lateral dynamics and parameter estimation of heavy vehicles[J]. *Mechanical Systems and Signal Processing*, 1998, 12(5): 611–626.

[18] VENTURE G, BODSON P, GAUTIER M, et al. Identification of the dynamic parameters of a car[J]. *SAE Technical Paper Series*, 2003: 2003-01-1283.

[19] LALTHLAMUANA R, TALUKDAR S. Obtaining vehicle parameters from bridge dynamic response: a combined semi-analytical and particle filtering approach[J]. *Journal of Modern Transportation*, 2015, 23(1): 55–66.

[20] HUH K, LIM S, JUNG J, et al. Vehicle mass estimator for adaptive roll stability control[J]. *SAE Technical Paper Series*, 2007: 2007-01-0820.

[21] KOULOCHERIS D V, DERTIMANIS V K, SPENTZAS C N. Parametric identification of vehicle's structural characteristic[J]. *Forsch Ingenieurwes*, 2008, 72(1): 39–51.

[22] ZHANG N, HAYAMA S. Identification of structural system parameters from time domain data (identification of global modal parameters of a structural system by the improved state variable method)[J]. *International Journal of the Japan Society of Mechanical Engineers Series 3*, 1990, 33(2): 168–175.

Biographical notes

ZHENG Minyi, born in 1983, is currently a PhD candidate at *State Key Laboratory of Advanced Design and Manufacture for Vehicle Body, Hunan University, China*. He received his master degree from *Hunan University of Science and Technology, China*, in 2011. His research interests include vehicle dynamics and parameter identification.
Tel: +86-18573156573; E-mail: zheng_minyi@163.com

ZHANG Bangji, born in 1967, is currently an associate professor at *State Key Laboratory of Advanced Design and Manufacture for Vehicle Body*, *Hunan University*, *China*. He received his PhD degree from *Hunan University*, *China*, in 2010. His research interests include vehicle NVH and mechanical system dynamics.
Tel: +86-731-88823072; E-mail: bangjizhang@hnu.edu.cn

ZHANG Jie, born in 1987, is currently a PhD candidate at *State Key Laboratory of Advanced Design and Manufacture for Vehicle Body*, *Hunan University*, *China*. He received his bachelor degree from *Jianghan Petroleum University*, *China*, in 2011. His research interest is vehicle system dynamics.
Tel: +86-13027484202; E-mail: zhangjie1906@sina.cn

ZHANG Nong, born in 1959, is currently a professor at *State Key Laboratory of Advanced Design and Manufacture for Vehicle Body, Hunan University, China*. He received his PhD degree from *The University of Tokyo*, Japan, in 1989. He has been involved in research in arears of dynamics and control of automotive systems including powertrains with various types of transmissions, hybrid propulsion systems, vehicle dynamics, passive and active suspensions; and mechanical vibration including experimental modal analysis, rotor dynamics, cold rolling mill chatter and machine condition monitoring.
E-mail: nong_zhang@163.com